

**Rational design of phenanthroimidazole derivative with hybridized
local and charge-transfer characteristics to achieve efficient blue
emission in non-doped OLED**

Jinnan Huo^{a,#}, Chenxi Gao^{a,#}, Yinpeng Cao^a, Heping Shi^{a,*}, Ben Zhong Tang^{b,*}

*^aSchool of Chemistry and Chemical Engineering, Shanxi University, Taiyuan
030006, China. E-mail: hepingshi@sxu.edu.cn*

*^bShenzhen Institute of Aggregate Science and Technology, School of Science and
Engineering, The Chinese University of Hong Kong, Shenzhen, Guangdong 518172,
China. Email: tangbenz@cuhk.edu.cn*

#Jinnan Huo and Chenxi Gao contributed equally to this article.

1. Syntheses

1.1 Synthesis of 9,9'-(5-bromo-1,3-phenylene) bis(9H-carbazole) (1)

Under nitrogen, the mixture of carbazole (12.53 g, 75 mmol), 1,3,5-tribromobenzene (11.78 g, 37.5 mmol), CuI (0.72 g, 3.75 mmol), 18-crown-6 (1.5 g, 35.7 mmol), potassium carbonate (27.5 g, 112.5 mmol), and *o*-dichlorobenzene (200 mL) were refluxed at 185 °C for 29 h. After cooling to room temperature, the mixture was quenched with water and extracted with chloroform. After washing, the mixture was dried with anhydrous magnesium sulfate. The white solid (20g, 60%) was obtained by column chromatography (petroleum ether: dichloromethane =6:1, v: v). ¹H NMR (400 MHz, CDCl₃) δ 8.09 (d, *J* = 8.7 Hz, 4H), 7.81 (d, *J* = 1.8 Hz, 2H), 7.74 (t, *J* = 1.9 Hz, 1H), 7.50 (d, *J* = 8.2 Hz, 4H), 7.44 – 7.38 (m, 4H), 7.28 (dd, *J* = 14.9, 1.1 Hz, 4H). ¹³C NMR (101 MHz, CDCl₃) δ 140.51, 140.34, 128.67, 126.42, 124.16, 123.96, 123.85, 120.82, 120.63, 109.65, 77.43, 77.11, 76.79. *m/z*: [M+H]⁺ calcd for C₃₀H₁₉BrN₂: 487.062, found 488.069.

1.2 Synthesis of 3,5-di(9H-carbazol-9-yl) benzaldehyde (2)

In a 300 mL round-bottom flask, compound 1 (5.20 g, 10.7 mmol) and 80 mL tetrahydrofuran (THF) were added under nitrogen atmosphere. Then *t*-BuLi (20.8 mL, 16.1 mmol) was slowly added with a syringe at -78 °C. The mixture was stirred at -78 °C for 1 h and then stirred at room temperature for 12 h. Subsequently, 5 mL *N,N*-dimethylformamide (DMF) was dropwised at -78 °C. The mixture was stirred at -78 °C for 1.5 h and then stirred for at room temperature 7 h. Then, 60 mL of concentrated hydrochloric acid (2 mol/L) was slowly added at -10 °C. The mixture was stirred at -10 °C for 1 h and then at room temperature for 12 h. The mixture was extracted with dichloromethane and dried in a vacuum oven for 12 h. The crude product was purified by column chromatography (dichloromethane: petroleum ether=2:1, v: v) to obtain 2.03 g yellow solid with yield of 44%. ¹H NMR (600 MHz, CDCl₃) δ 10.22 (s, 1H), 8.23 (s, 2H), 8.18 (s, 4H), 8.13 (s, 1H), 7.54 (d, *J* = 5.3 Hz, 4H), 7.47 (s, 4H), 7.35 (s, 4H).

1.3 Synthesis of 3',5'-di(9H-carbazol-9-yl)-[1,1'-biphenyl]-4-carbaldehyde (3)

In a 300 mL volumetric flask, compound 1 (5.278 g, 10.86 mmol), 50 ml toluene, 50 ml THF, 20 ml H₂O, 4-formylphenylboronic acid (1.95 g, 13 mmol), potassium carbonate (5.99 g, 43.44 mmol) and tetrakis(triphenylphosphine)palladium (0) (2.4 g, 1.73 mmol) were added to the system at 120°C under nitrogen and stirred overnight. The crude product was purified by column chromatography (dichloromethane: petroleum ether = 1:2, v: v) to obtain a white powder (4.187 g, 75%). m/z: [M+H]⁺ calcd for C₃₇H₂₄N₂O: 512.189, found 513.179.

1.4 Synthesis of 4-(2-(3,5-di(9H-carbazol-9-yl) phenyl)-1H-phenanthro[9,10-d]imidazol-1-yl) benzonitrile (DCCPPI).

Under the protection of nitrogen, the mixture of 9-10 phenanthrenequinone (0.8015 g, 3.85 mmol), 4-aminobenzonitrile (2.273 g, 19.26 mmol), compound 2 (1.68 g, 3.85 mmol), ammonium acetate (2.97 g, 38.53 mmol) and 120ml glacial acetic acid was refluxed at 125 °C for 29 h. After cooling to room temperature, the mixture was poured into methanol solution and stirred, and then washed with ethanol solution (ethanol: water = 1:1, v: v) after suction filtration. The crude product was purified by column chromatography (petroleum ether: dichloromethane =1:3, V: V) and washed with ethanol to produce a yellow solid. Yield: 3.71 g (82.3%). ¹H NMR (600 MHz, CDCl₃) δ 8.94 (d, *J* = 7.4 Hz, 1H), 8.78 (d, *J* = 8.5 Hz, 1H), 8.70 (d, *J* = 8.2 Hz, 1H), 8.19 – 8.11 (m, 4H), 8.02 (d, *J* = 8.5 Hz, 2H), 7.91 (d, *J* = 2.0 Hz, 2H), 7.85 (t, *J* = 1.9 Hz, 1H), 7.79 (dd, *J* = 23.2, 8.4 Hz, 3H), 7.72 – 7.68 (m, 1H), 7.57 (t, *J* = 8.4 Hz, 1H), 7.48 (t, *J* = 8.3 Hz, 4H), 7.37 – 7.31 (m, 9H), 6.99 (d, *J* = 10.1 Hz, 1H). ¹³C NMR (151 MHz, CDCl₃) δ 140.62, 140.12, 135.03, 130.61, 130.22, 128.94, 128.50, 128.27, 127.19, 127.03, 126.66, 126.32, 124.92, 124.06, 123.55, 122.34, 121.13, 120.92, 117.77, 115.12, 109.82. m/z: [M]⁺ calcd for C₅₂H₃₁N₅: 726.258, found: 726.263.

1.5 Synthesis of 4-(2-(3',5'-di(9H-carbazol-9-yl)-[1,1'-biphenyl]-4-yl)-1H-phenanthro[9,10-d]imidazol-1-yl) benzonitrile (DCBCPPI).

DCBCPPI was synthesized from 9,10-phenanthrenequinone (0.8015 g, 3.853 mmol), 4-aminobenzonitrile (2.273 g, 19.265 mmol), compound 3 (1.975 g, 3.853

mmol), ammonium acetate (2.97 g, 38.53 mmol) and 160ml glacial acetic acid by followed the same 1.4 process, resulting in a white solid in 31% yield (0.967 g, 1.21 mmol). ¹H NMR (600 MHz, CDCl₃) δ 8.89 (s, 1H), 8.75 (d, *J* = 8.0 Hz, 1H), 8.67 (d, *J* = 8.2 Hz, 1H), 8.18 (d, *J* = 7.8 Hz, 4H), 7.98 – 7.86 (m, 4H), 7.83 (s, 1H), 7.77 (t, *J* = 7.4 Hz, 1H), 7.71 (d, *J* = 8.1 Hz, 2H), 7.69 – 7.60 (m, 5H), 7.59 (d, *J* = 8.2 Hz, 4H), 7.54 – 7.46 (m, 5H), 7.33 (dt, *J* = 21.6, 7.5 Hz, 5H), 7.09 (d, *J* = 7.8 Hz, 1H). ¹³C NMR (101 MHz, CDCl₃) δ 144.01, 141.17, 140.55, 134.75, 130.81, 130.19, 129.06, 128.27, 127.82, 127.23, 126.87, 125.07, 124.91, 124.27, 123.77, 121.17, 121.10, 118.14, 114.87, 114.81, 110.24. m/z: [M]⁺ calcd for C₅₈H₃₅N₅: 801.953, found: 801.957.

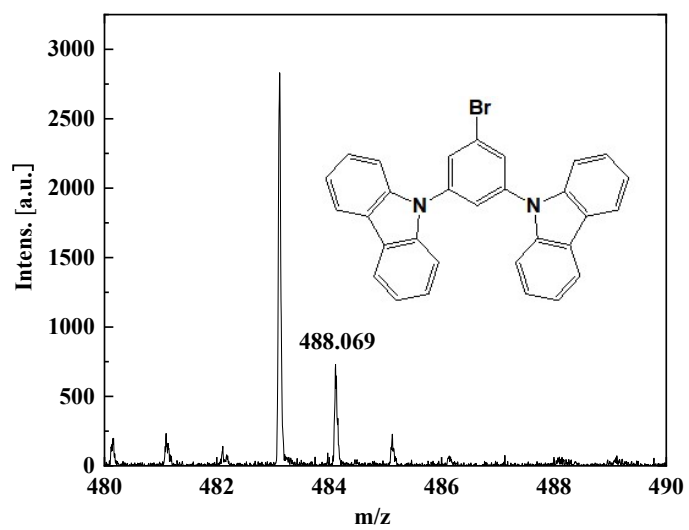
2. General Characterization

¹HNMR and ¹³CNMR were measured on Bruker 400 MHz narrow cavity liquid nuclear magnetic resonance instrument. High-resolution mass spectra (HRMS) were recorded on Autoflex III (MALDI-TOF-MS). UV spectra were obtained on a Shimadzu UV-2450 absorption spectrophotometer. Fluorescence measurements were performed on a Shimadzu RF-5301PC fluorescence spectrometer. Thermogravimetric analysis (TGA) was carried out on TGA 2050 thermogravimetric analyzer under nitrogen at a heating rate of 10 °C min⁻¹ from room temperature to 600 °C. All the transition density matrix calculations in this paper are done through the Gaussian09 software package. The ground-state geometries were optimized using the density function theory (DFT) method with M06-2X hybrid functional at the basis set level of 6-31G (d, p). The geometry and energy levels of the excited state were performed using td- M06-2X/6-31g (d, p) level. All emission natural transition orbitals (NTOs) of S_n→S₀ and T_n→S₀ were performed at td- M06-2X/6-31g (d, p). The resulting transition density matrix data is plotted by the Multiwfn software to obtain a two-dimensional color map of electron-hole pairs. Cyclic voltammetry (CV) was measured using glassy carbon electrode as the working electrode, Ag/Ag⁺ (0.01 M AgNO₃) electrode as the reference electrode and Pt wire as the counter electrode. Sufficient nitrogen is injected into the electrolytic cell prior to testing. The electrolyte

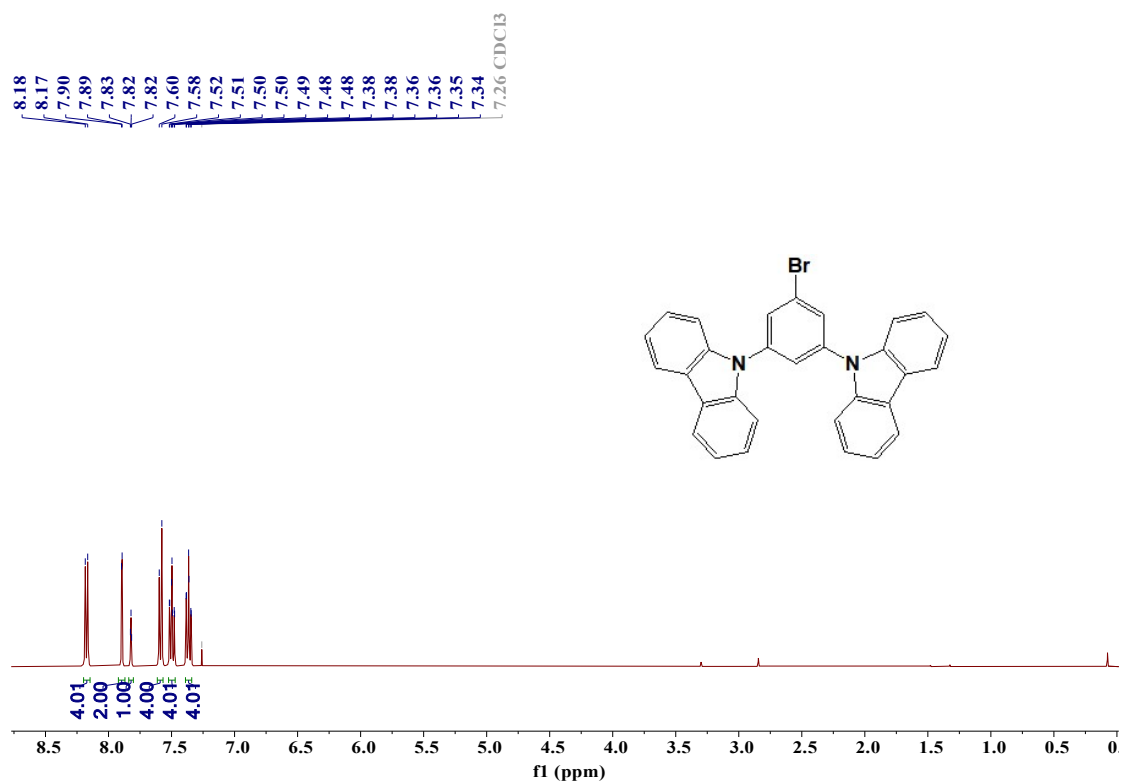
was 0.1 mol L⁻¹ of tetrabutylammonium hexafluorophosphate, and the scan speed was 50 mV s⁻¹. The solvent scanned was dry anhydrous dichloromethane. The energy level is obtained based on the starting oxidation potential. The corrected PLQY was obtained by manual operation using an integrating sphere device. The phosphorescence lifetimes were measured using an Edinburgh Instruments F980 spectrometer.

3. Device fabrication and measurements

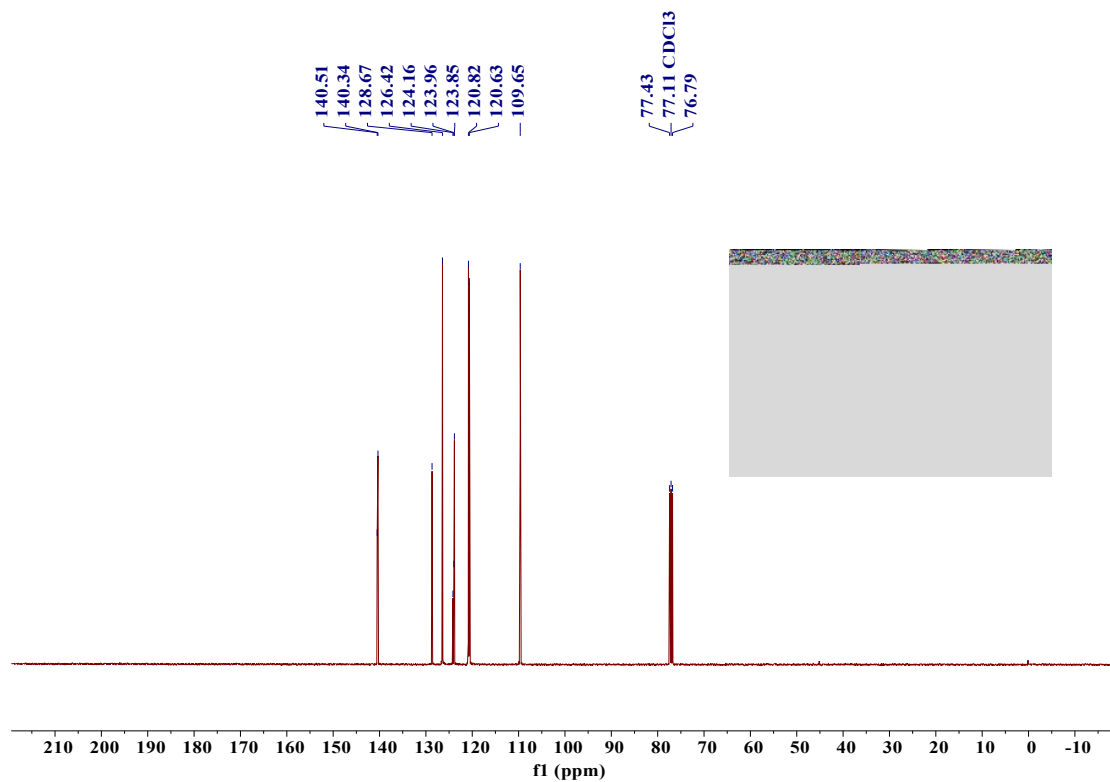
Multi-layer OLEDs are prepared by thermal evaporation under high vacuum (5×10^{-4} Pa) pre-coated on glass (3×3 mm) with an ITO layer as the anode. The constructions of these devices are ITO/ HATCN (20 nm)/ TAPC (40 nm)/ emitting layers (20 nm)/ TPBi (40 nm)/ LiF (1.5 nm)/ Al (100 nm). 1,4,5,8,9,11-hexaazatriphenylenehexacarbonitrile (HATCN) serves as hole injection layer (HIL), 4,4'-cyclohexylidenebis [*N*, *N*-bis(*p*-tolyl) aniline] (TAPC) serves as the hole transport layer (HTL), 1,3,5-tris(1-phenyl-1*H*-benzimidazol-2-yl) benzene (TPBi) serves as electron transport layer (ETL). The evaporation rates of HIL, HTL, EML, and ETL are 0.3 Å s⁻¹, 0.3 Å s⁻¹, 0.4 Å s⁻¹, 0.3 Å s⁻¹, respectively. The evaporation rate of cathode Al ranges from slow to gradually faster to 10.0 Å s⁻¹. The functional layers were sequentially vapor-deposited at a temperature of 300-320 °C. The current/voltage of the device is determined by Keithley 2400, and the brightness and EL spectrum are determined by CS 200. Testing of the devices is performed in air at room temperature.



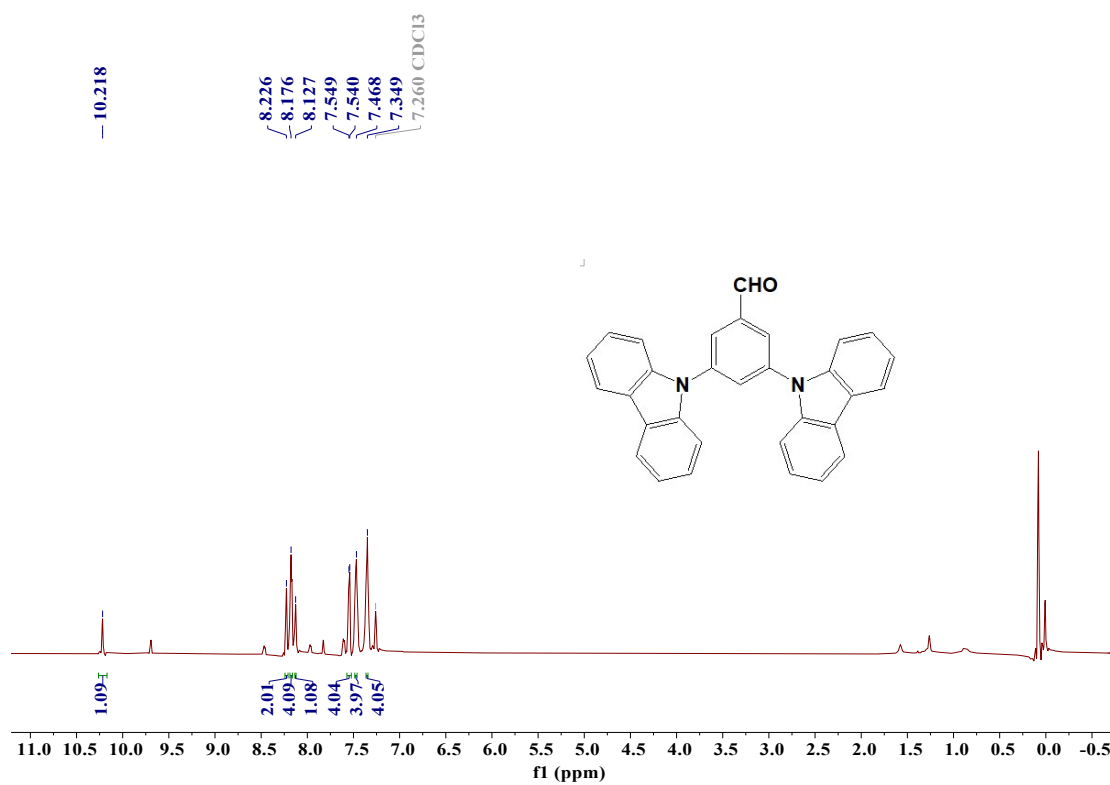
Mass spectrometry of compound 1



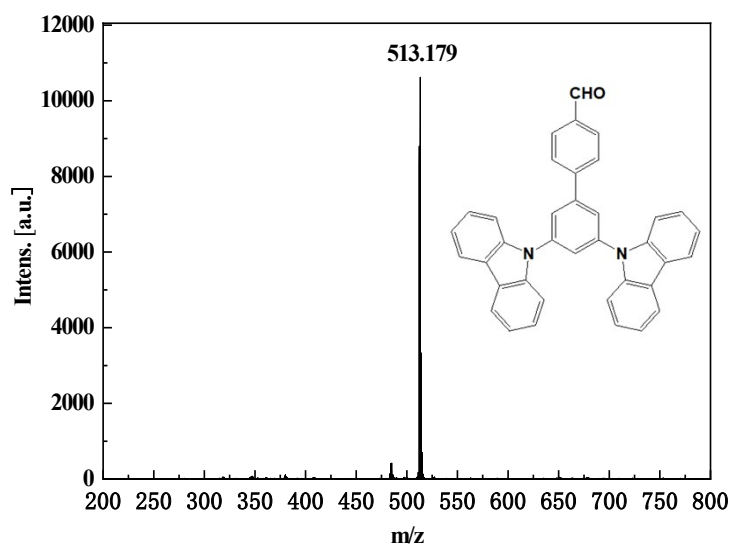
¹H-NMR of compound 1



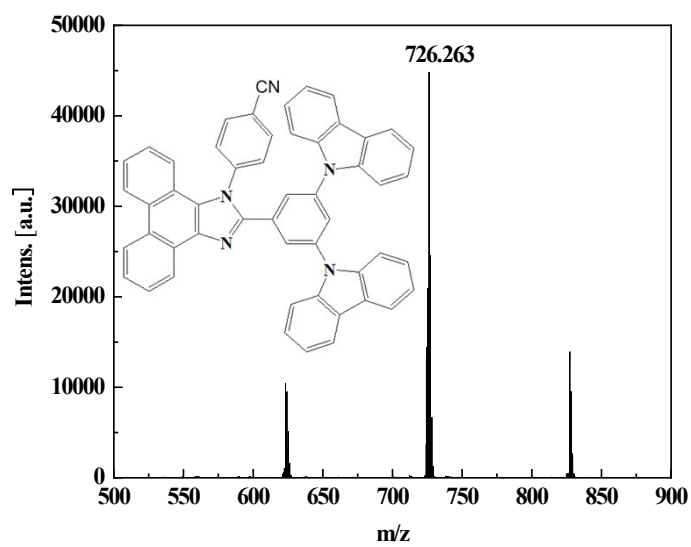
¹³C NMR of compound 1



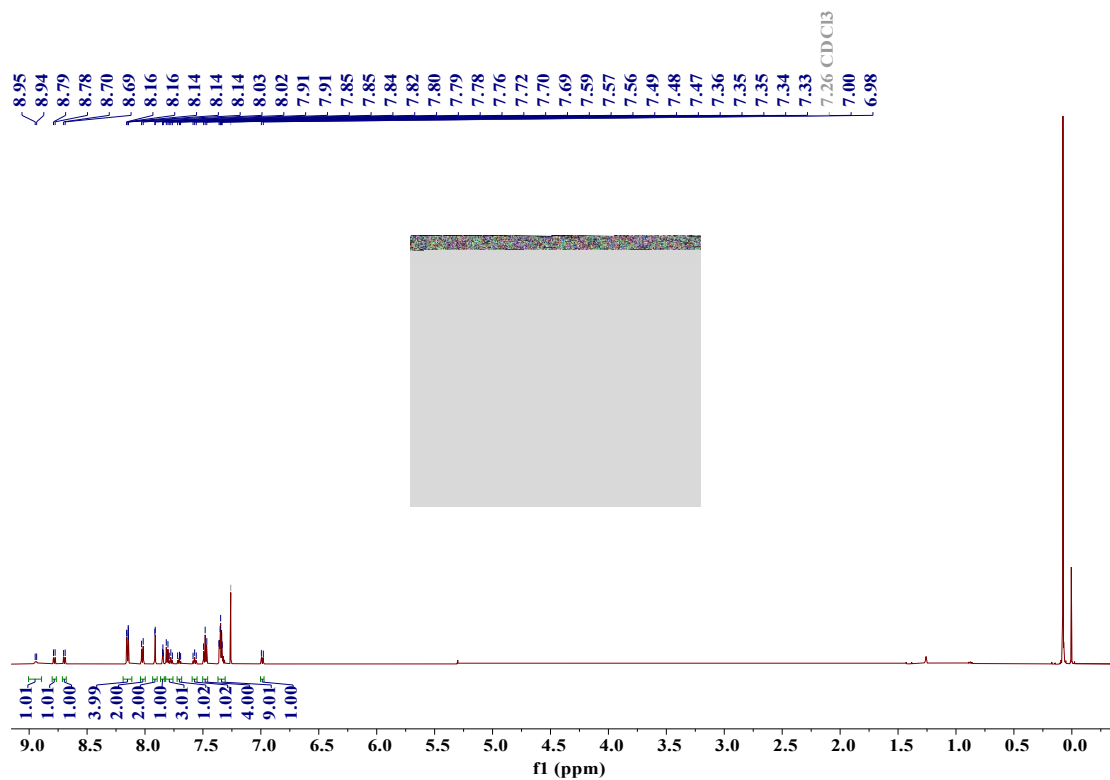
¹H-NMR of compound 2



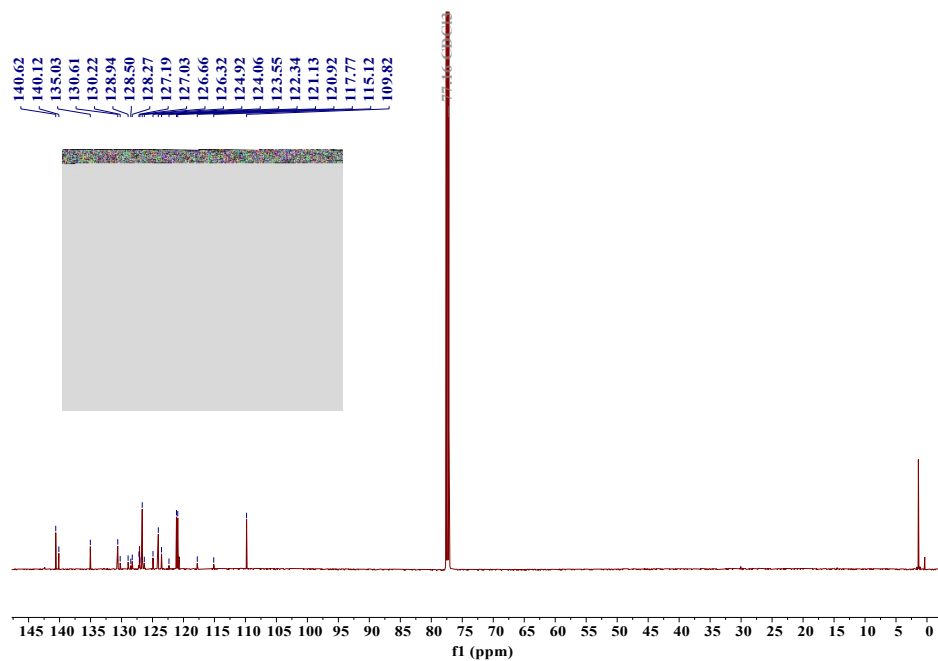
Mass spectrometry of compound 3



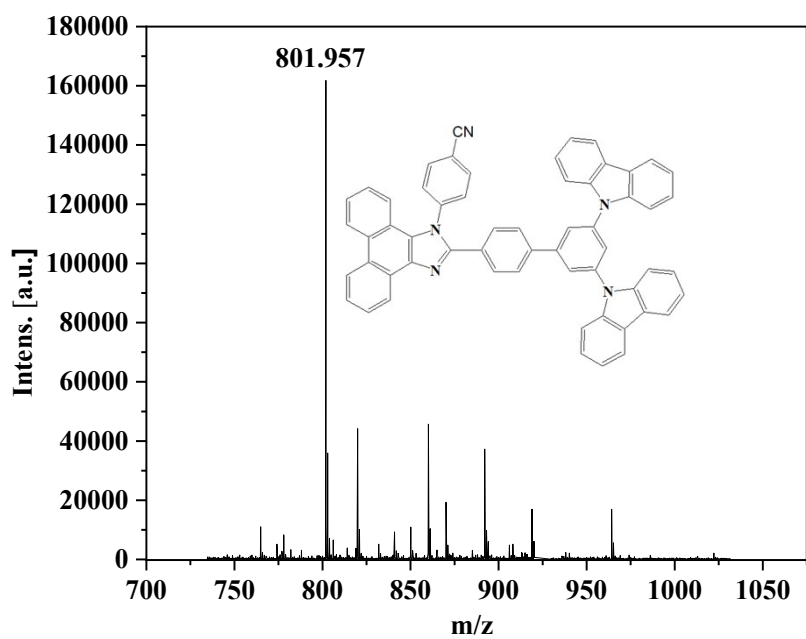
Mass spectrometry of DCCPPI



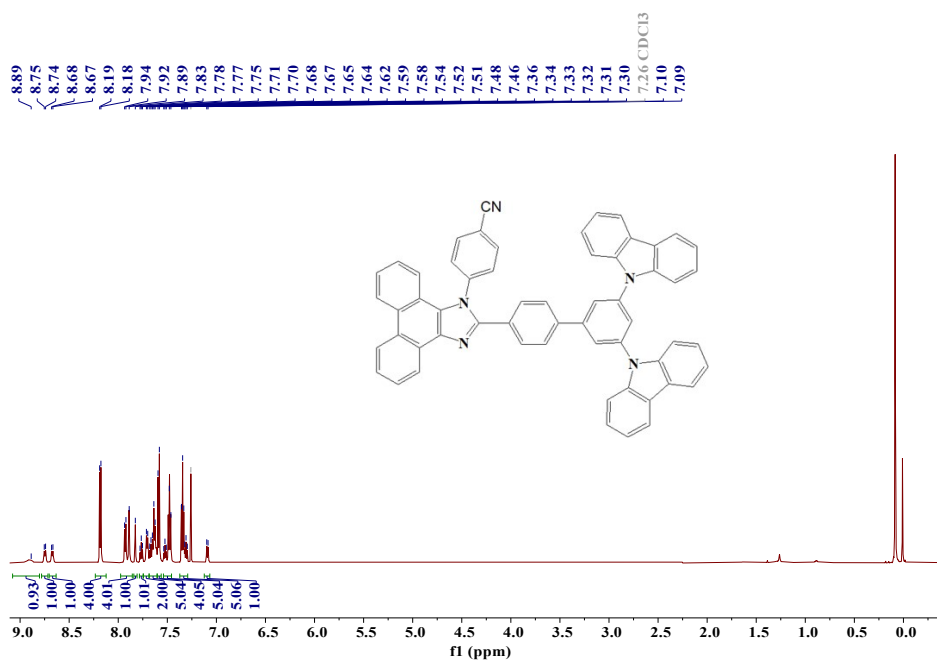
¹H NMR of DCCPPI



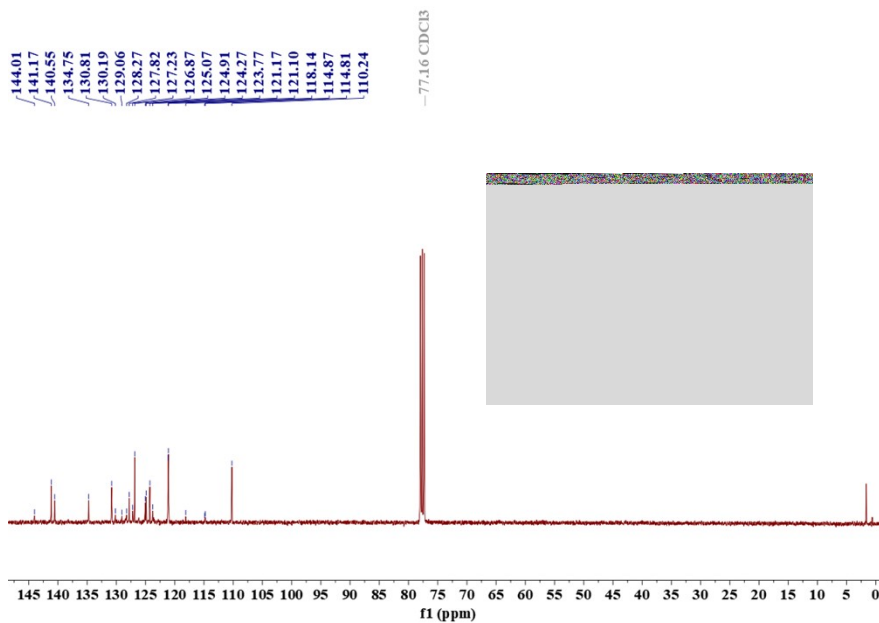
¹³C NMR of DCCPPI



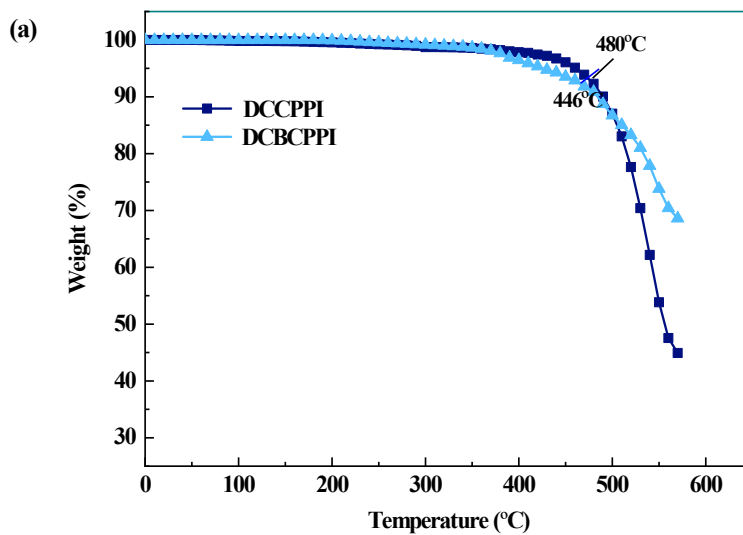
Mass spectrometry of **DCBCPPI**



¹H NMR of **DCBCPPI**



¹³C NMR of DCBCPPI



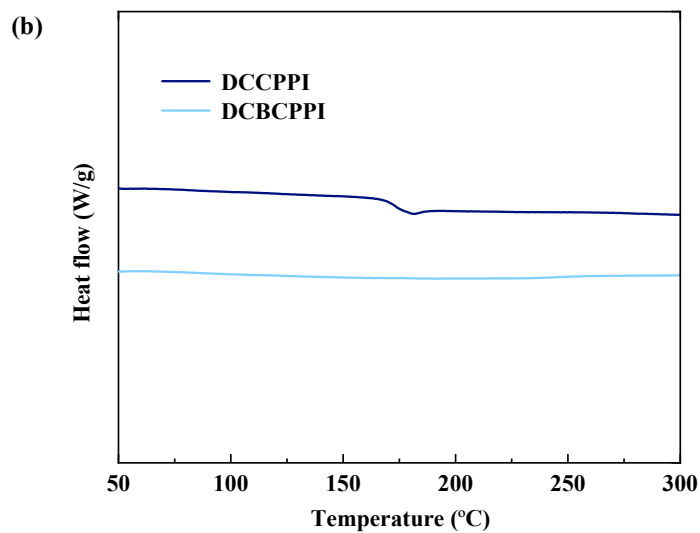
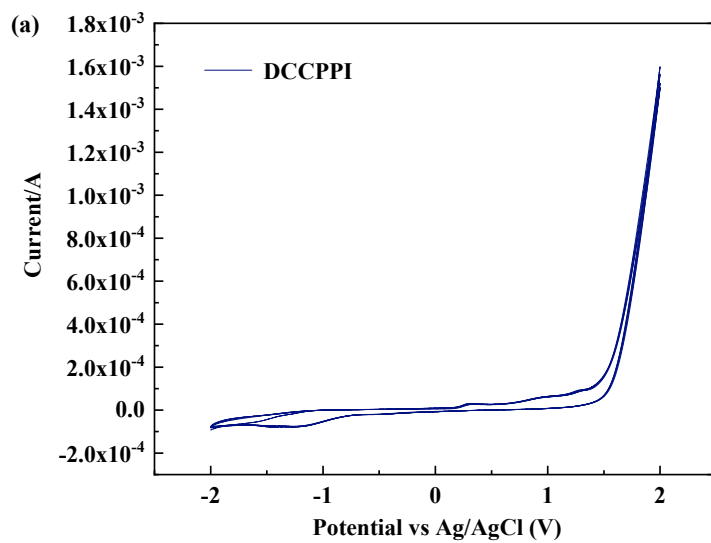


Fig. S1 (a) TGA curves and (b) DSC curves of **DCCPPI** and **DCBCPPI**.



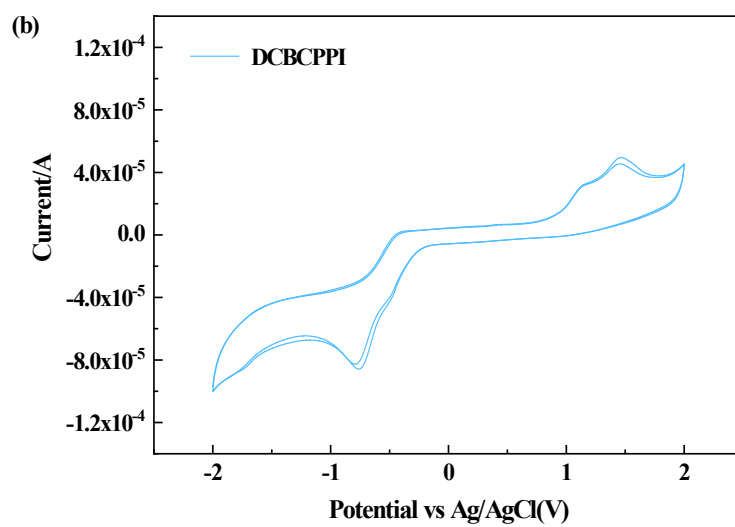


Fig. S2 Cyclic voltammograms of (a) DCCPPI and (b) DCBCPPI.

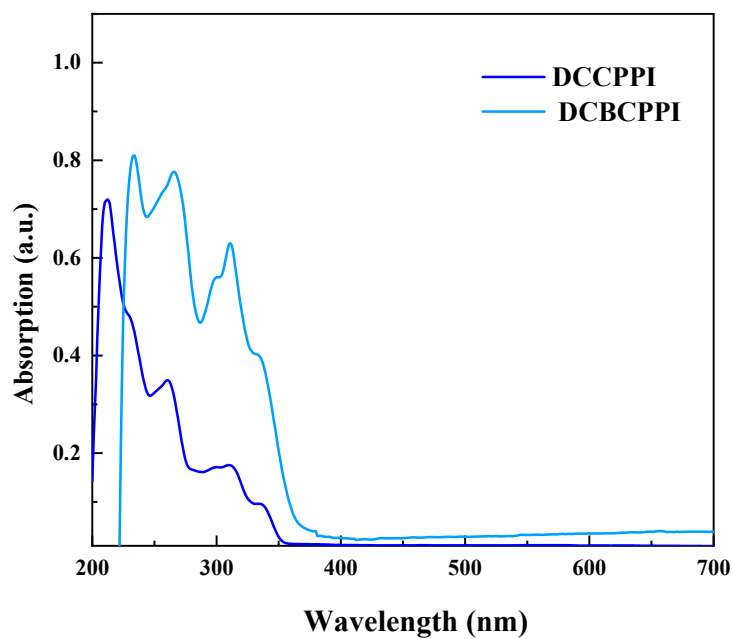
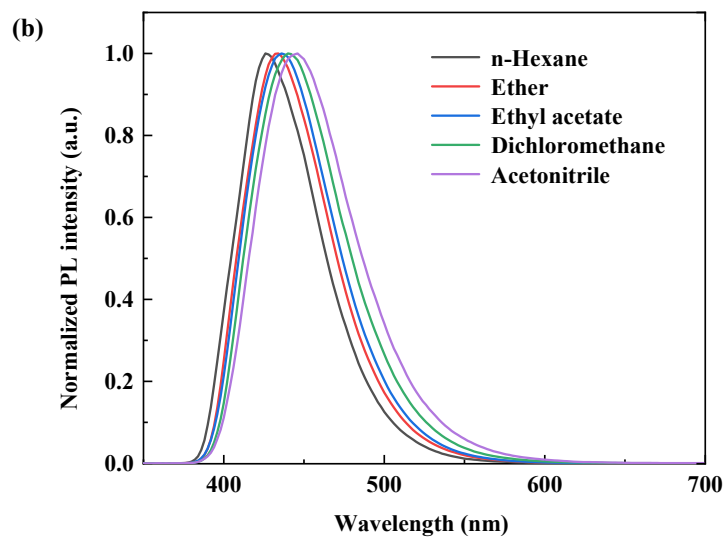
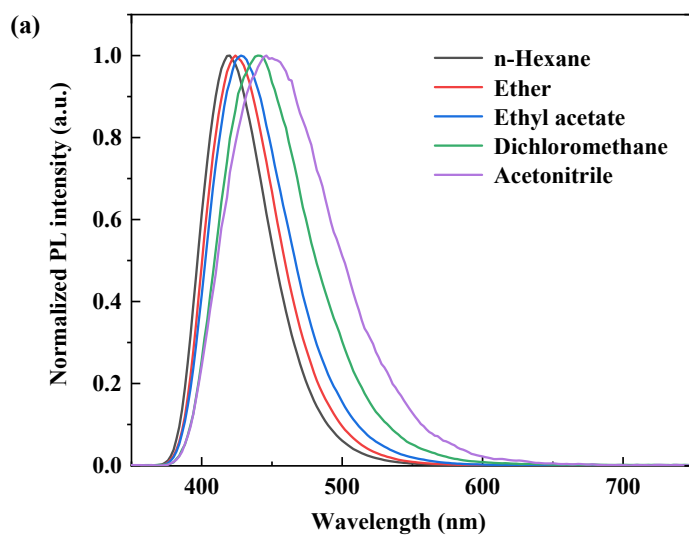


Fig. S3 The UV-vis absorption spectra of DCCPPI and DCBCPPI in film.



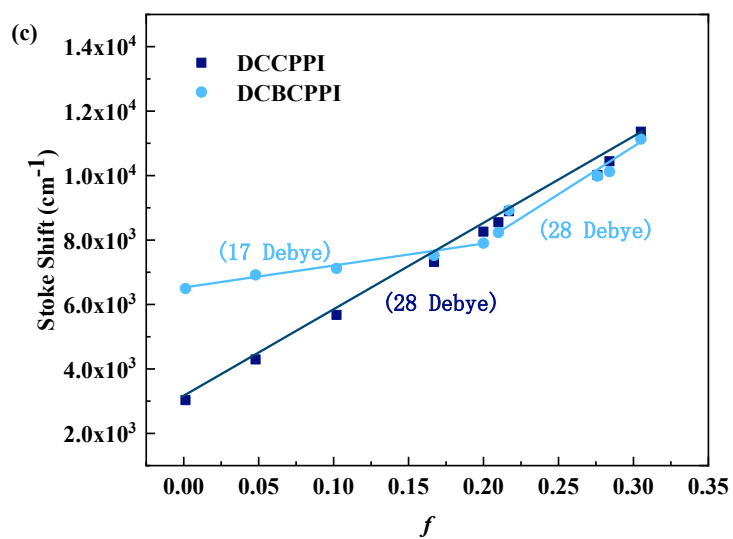
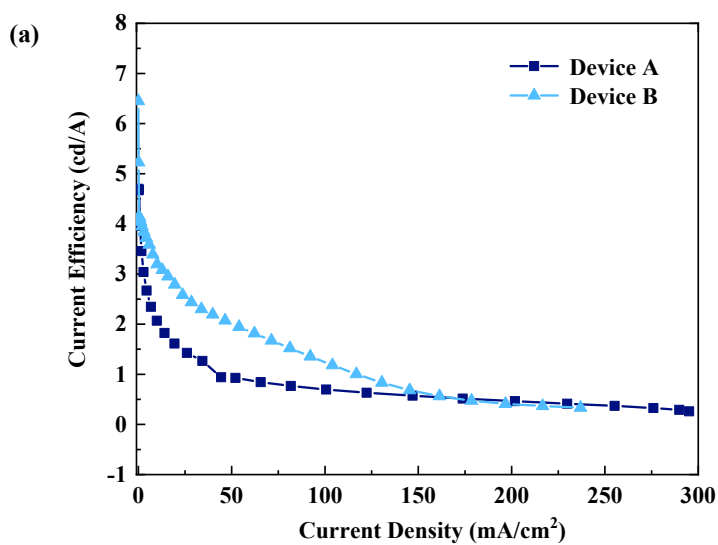


Fig. S4 The PL spectra of (a) **DCCPPI** and (b) **DCBCPPI** in different diluted solutions and the (c) Lippert-Mataga solvatochromic model.



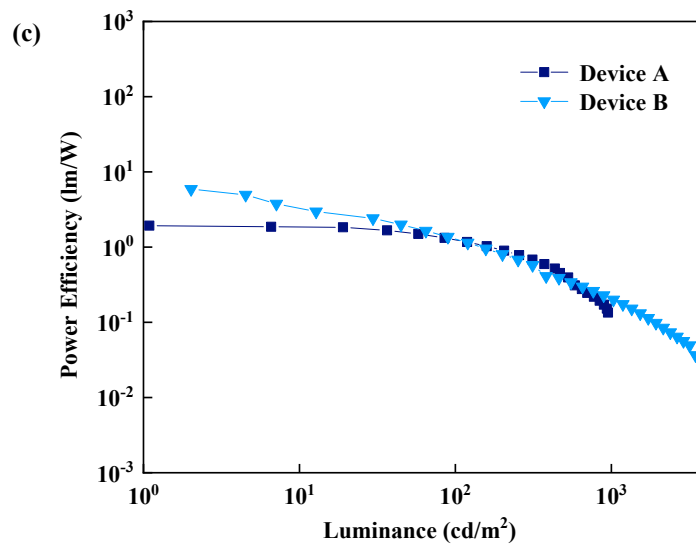
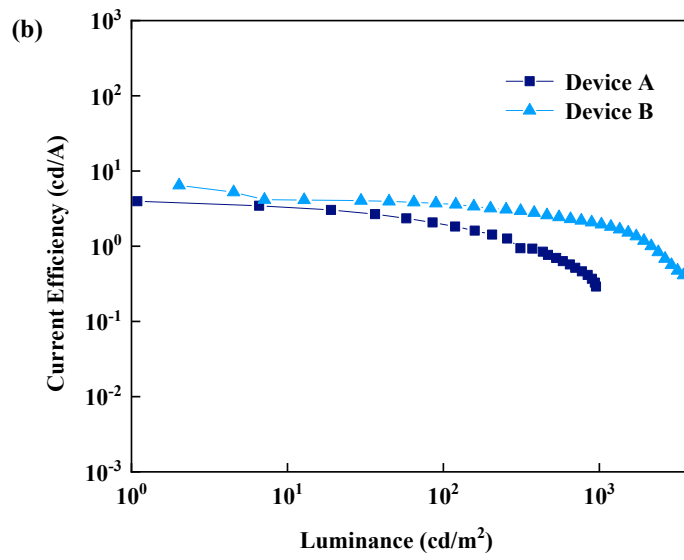


Fig. S5 (a) Current efficiency–current density characteristics, (b) current efficiency–luminance characteristics, (c) power efficiency–luminance characteristics of devices A and B.

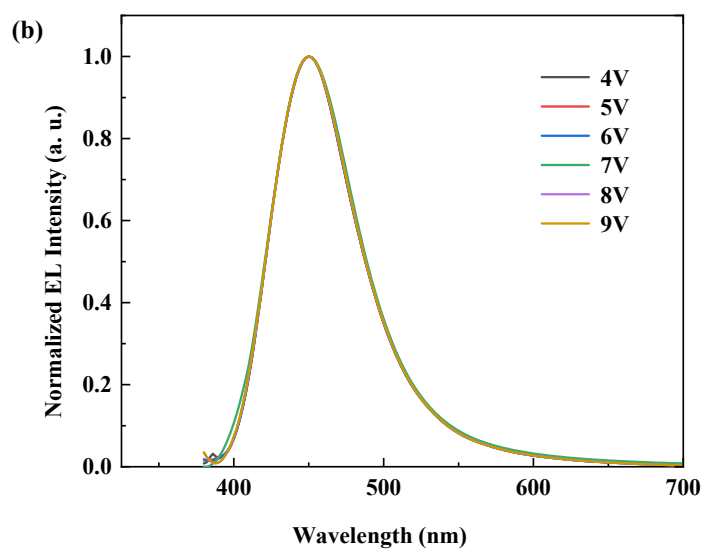
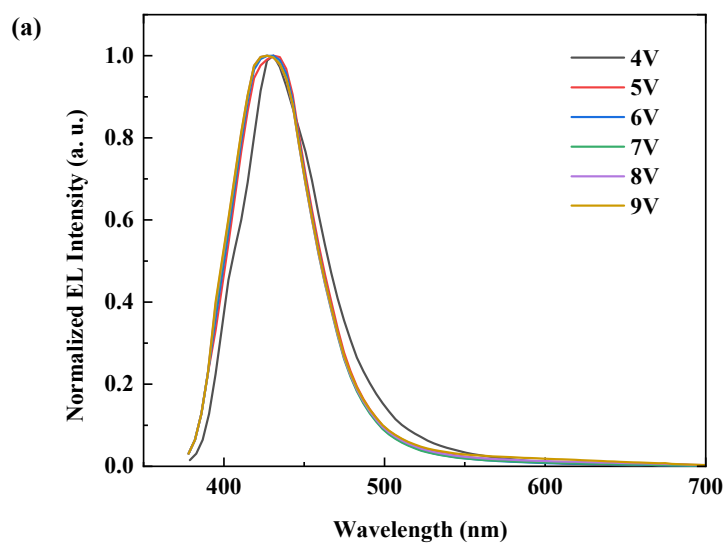
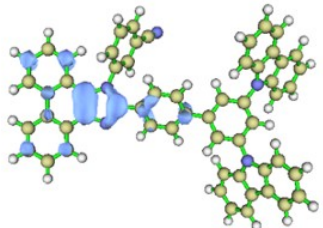
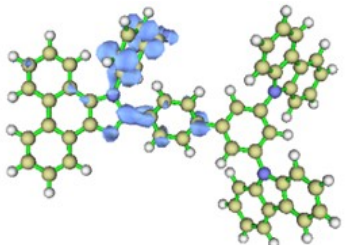
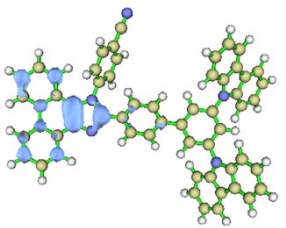
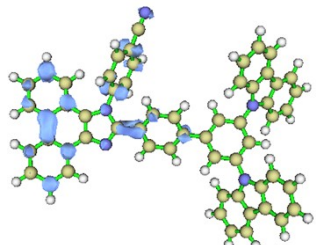
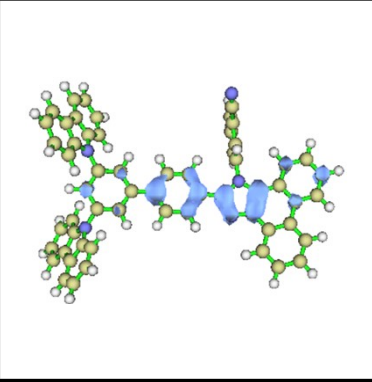
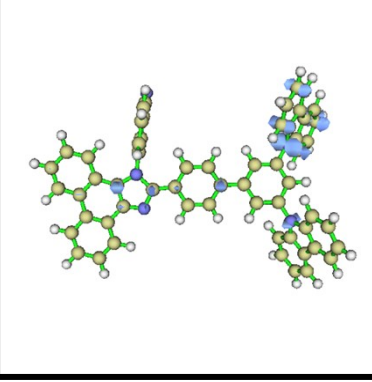


Fig. S6 Normalized EL intensity with different voltages of devices (a) A and (b) B.

Table S1 NTOs of DCBCPPI.

	Energy	f	Transition Character	Hole	Particle	Molecular Orbital Transition Contribution	Δr
$S_0 \rightarrow S_1$	2.773	0.0276	HLCT			96.6%	3.8 Å
$S_0 \rightarrow S_2$	2.940	0.0048	HLCT			85.2%	3.5 Å

$S_0 \rightarrow T_1$	1.988	0.0000	LE		91.4%	2.7 Å
$S_0 \rightarrow T_5$	2.970	0.0000	CT		55.4%	4.4 Å